Geomicrobiology Journal (2015) **32**, 130–139

ISSN: 0149-0451 print / 1521-0529 online
DOI: 10.1080/01490451.2014.933287

Taylor & Francis
Taylor & Francis Group

Clostridium Species as Metallic Copper-Forming Bacteria in Soil under Reducing Conditions

ANKE F. HOFACKER[1], SEBASTIAN BEHRENS[2]*, ANDREAS VOEGELIN[3], RALF KAEGI[3], TINA LÖSEKANN-BEHRENS[2], ANDREAS KAPPLER[2], and RUBEN KRETZSCHMAR[1]*

[1]*Soil Chemistry Group, Institute of Biogeochemistry and Pollutant Dynamics, ETH Zurich, Zurich, Switzerland*
[2]*Geomicrobiology, Center for Applied Geosciences, University of Tübingen, Tübingen, Germany*
[3]*Eawag, Swiss Federal Institute of Aquatic Science and Technology, Dübendorf, Switzerland*

Received October 2013, Accepted June 2014

Recent studies have reported the formation of Cu^0 nanoparticles (CuNP) by suspended bacteria in pore water of periodically flooded soils, but the bacteria have not yet been identified. The aim of this study was to identify the CuNP-forming bacteria and to determine the location of CuNP formation relative to the bacterial cell surface. Electron microscopy revealed that the bacteria were rod-shaped spore formers and suggested that CuNP were formed in the periplasm. Combined results from denaturing gradient gel electrophoresis, 16S rRNA gene clone libraries, and classic microbiological cultivation techniques provided strong evidence for a *Clostridium* sp. strain as the CuNP-forming bacteria. Clostridia are well-adapted to frequent flooding and drying due to their ability to form spores and may play an important role in Cu cycling and metallic Cu formation in redox-dynamic environments.

Keywords: biomineralization, Clostridia, *copA*, copper, metals, nanoparticles, molecular microbial ecology, redox, soil, spore forming bacteria, wetland

Introduction

In many regions worldwide, riparian floodplain soils are affected by the accumulation of Cu and other potentially toxic trace elements released to the environment by anthropogenic activities including mining, smelting, and industry. Periodic flooding of riparian soils induces changes in soil redox conditions that affect the speciation and mobility of trace elements (Weber et al. 2009b), potentially leading to their release into surface waters and groundwater (Hofacker et al. 2013a; Hofacker et al. 2013b; Weber et al. 2009a). In laboratory microcosm experiments with contaminated floodplain soil, we observed that soil flooding led to Cu^{2+} reduction to Cu^+ and to the formation of metallic Cu^0 as long as microbial sulfate reduction was limited (Weber et al. 2009b). Reductive Cu transformation was accompanied by colloidal Cu mobilization into the soil pore water in the form of metallic Cu^0 nanoparticles (referred to herein as CuNP) associated with suspended bacteria (Hofacker et al. 2013b; Weber et al. 2009a). These findings point towards an active role of bacteria in CuNP formation. Biomineralization of CuNP was attributed to Cu^+ export from bacterial cells via a Cu homeostasis reaction followed by Cu^+ disproportionation near the cell (Weber et al. 2009a). Metallic Cu was recently also observed to form during anoxic incubation of a Cu-spiked paddy soil (Fulda et al. 2013), indicating that metallic Cu formation by bacteria may be a common process in periodically flooded soils. However, the type of bacteria involved in this process and the exact location of CuNP formation relative to the bacterial cell surface are not known to date.

In prokaryotes, Cu serves as an important cofactor in several classes of proteins including electron transfer proteins, hydrolytic and redox enzymes, oxygen transporters, and proteins in signaling pathways, due to its ability to undergo reversible redox changes between Cu^+ and Cu^{2+} (Banci et al. 2010). Copper can be highly toxic to cells, especially when present as free metal ion in the cytoplasm. Reactive oxygen species (ROS) known to play an important role in oxidative damage of bacterial DNA have been shown to damage *Escherichia coli* cells mainly via Cu^{2+} to Cu^+ reduction and Cu^+ cytotoxicity (Park et al. 2012). A mechanistic study on Cu toxicity showed the inactivation of the 4Fe-4S cluster of dehydratases (essential in the tricarboxylic acid (TCA) cycle and amino acid synthesis) via Cu^+ ligation to the coordinating sulfur atoms, leaving the Fe to react in a Fenton reaction under the production of $^{\bullet}OH$ radicals damaging the DNA of the cells (Macomber and Imlay 2009). To avoid toxic side reactions, cells have developed homeostatic systems to

*Address correspondence to Sebastian Behrens, Center for Applied Geosciences, University of Tübingen, Sigwartstrasse 10, D-72076 Tübingen, Germany; Email: sebastian.behrens@ifg.uni-tuebingen.de or to Ruben Kretzschmar, Institute of Biogeochemistry and Pollutant Dynamics, CHN, ETH Zurich, CH-8092 Zurich, Switzerland; Email: kretzschmar@env.ethz.ch
Color versions of one or more of the figures in the article can be found online at www.tandfonline.com/ugmb

maintain low levels of intracellular Cu (Finney and O'Halloran 2003; Outten et al. 2001). Chaperones in the cytoplasm or periplasm of prokaryotic cells scavenge and deliver Cu to specific Cu^+ efflux pumps (Tottey et al. 2005). P_{1B}-type ATPases are common Cu^+ transmembrane efflux pumps (CopA) coupling the energy provided by ATP hydrolysis to the efflux of cytoplasmic substrates (Arguello et al. 2007; Osman and Cavet 2008; Solioz et al. 2010). CopA in *E. coli* was among the first that was fully characterized (Rensing et al. 2000). Bacterial detoxification mechanisms were also shown to be important in Au^0 nanoparticle formation by *Cupriavidus metallidurans* CH34 (Reith et al. 2009). Bacterially formed intra- and extracellular metallic nanoparticles have been observed mainly for Au and Ag (Narayanan and Sakthivel 2010), whereas reports for CuNP are limited. Large networks of spear-shaped Cu(0) crystals have been suggested to form by reaction of Cu^{2+} with waste products of bacterial metabolism (Lovering 1927) and *Pseudomonas stutzeri* was proposed to produce CuNP (Varshney et al. 2010). Formation of CuNP associated with plant roots has been attributed to endomycorrhizal fungi (Manceau et al. 2008).

The objectives of this study were (i) to determine whether the CuNP are formed at the outermost cell wall, inside the periplasm, or in the cytoplasm, (ii) to identify the CuNP-forming bacteria in the pore water of a metal-contaminated riparian floodplain soil, and (iii) to investigate the genetic potential for Cu detoxification in the identified bacteria. We performed soil microcosm experiments at temperatures between 5 and 23°C, and analyzed bacteria suspended in the pore water with electron microscopy and molecular microbiology techniques. Specifically, we used 16S rRNA gene-based denaturing gradient gel electrophoresis (DGGE) to follow microbial community shifts at different incubation temperatures over time and constructed a 16S rRNA gene clone library for more in-depth analysis of the microbial community composition. Furthermore we isolated spore forming bacteria from pore water samples, identified the isolates by 16S rRNA gene sequence analysis and tested the obtained isolates for the presence of genes encoding *copA*-type Cu^+ efflux pumps.

Materials and Methods

Soil Microcosm Experiments

Soil microcosm experiments were performed with topsoil material (0–15 cm) collected from a weakly acidic Gleyic Fluvisol in the floodplain of the river Mulde, Germany (Hofacker et al. 2013b; Weber et al. 2009a; Weber et al. 2009b). The Mulde floodplain is contaminated due to historic mining, smelting, and industry. The topsoil batch used in the present study (soil II) contained 160 mg/kg Cu, 11 mg/kg Cd, 374 mg/kg Pb, and 0.9 mg/kg Hg (Hofacker et al. 2013a), similar to another topsoil batch (soil I) from the same site (Hofacker et al. 2013b; Weber et al. 2009a; Weber et al. 2009b).

Flooding experiments for different types of analyses were conducted following the slightly different procedures A and B: (Procedure A) To obtain pore water and soil samples for DGGE and 16S rRNA gene clone library analysis, 550 g air-dried and sieved soil (200–2000 μm aggregate size; soil II) were equilibrated with 1500 mL artificial floodwater (0.6 mM NaCl, 0.6 mM $CaCl_2$, and 0.3 mM $Mg(NO_3)_2$) for 2 hours and centrifuged at 600 *g* for 15 min. The wet soil paste was transferred to 1 L polyethylene (PE) bottles open to the atmosphere and equipped with a suction cup (sintered PE granulate, 10–16 μm pore diameter; ~3.5 cm below soil-supernatant interface) and was flooded with 500 mL artificial floodwater (9 cm soil layer, 6 cm supernatant). The microcosms were incubated in the dark at 5, 14, or 23°C for up to 34 days.

(Procedure B) For the isolation of spore forming pore water bacteria for 16S rRNA gene and *copA* gene analysis as well as for the collection of pore water bacteria for transmission and scanning electron microscopy, 550 g dry soil and 700 mL artificial floodwater were placed into the microcosm and mixed to remove enclosed air (10 cm soil layer, 4 cm supernatant). These microcosms were incubated at 23°C for 4 days (highest colloidal Cu concentration). Further experimental details for each microcosm and an overview over the performed analyses are provided in Supplementary Table S1.

Sampling of Pore Water, Colloids, and Soil Solids

Pore water was sampled through the suction cups directly into an anoxic glovebox (MBraun MB 200B, M. Braun, Germany, < 10 ppm O_2) using a low flow rate (0.4 mL/min) to avoid colloid mobilization by shear forces. All pore water and colloid processing was performed within the glovebox. Unfiltered aliquots were taken before passing half of the remaining solution through 0.025 μm cellulose nitrate membrane filters (NC03; Whatman; Germany) and the other half through 0.22 μm polyethersulfone (PES) membrane filters at flow rates of 0.2 and 0.5 mL/min, respectively. Unfiltered and filtered aliquots were acidified to 0.5 M HCl and stored at 4°C until analysis by ICP-OES. Dissolved and colloidal Cu concentrations for individual microcosms are listed in Supplementary Table S1. For investigation of colloids by scanning electron microscopy (SEM), 10 mL of pore water were passed through Au sputter coated 0.2-μm polycarbonate (PC) membrane filters (Nuclepore). Another 10 mL of pore water were passed through 0.22-μm PES membrane filters, which were frozen and stored at −20°C for DNA extraction. For soil microbial DNA extraction, the microcosms were frozen in liquid N_2 and a 3-cm thick slice was cut around the suction cup with a diamond saw.

Transmission and Scanning Electron Microscopy

Colloids from 1.5 mL of unfiltered pore water were ultracentrifuged for 15 min at 2300 *g* and 60 min at 14300 *g* onto transmission electron microscopy (TEM) 400-mesh Ni grids (Formvar carbon reinforced, SPI Supplies, USA). The samples were investigated with a TEM (CM30, FEI, USA) operated with a LaB_6 source at 300 kV accelerating voltage. Images were recorded in bright field mode using

a CCD camera. The elemental composition of selected particles was determined by energy-dispersive X-ray (EDX) spectrometry (Noran System Six; Thermo, USA). The same grids were investigated in a SEM (Nova NanoSEM 230, FEI) to quantify the bacteria with cell-associated CuNP relative to the total number of cells. The SEM was equipped with a transmission electron detector and bright field images were recorded. Elemental analysis was performed with an EDX system (INCA, Oxford, UK) attached to the microscope.

For high-resolution SEM analysis, suspended pore water bacteria were collected on 0.2-μm Au-coated PC membrane filters (Nuclepore 25 mm). Subsequently, the bacteria on the filters were fixed in 2.5% glutaraldehyde for 5 days under N_2 atmosphere in glass vials in gas-tight Al bags at 4°C. Filters were washed twice in 1x PBS (phosphate buffered saline: 137 mM NaCl, 2.7 mM KCl, 10 mM Na_2HPO_4, 2 mM KH_2PO_4) in the glovebox by replacing the solution carefully with a syringe. Afterwards, the bacteria on the filter were dehydrated by an ascending ethanol series (15, 30% ethanol in 1x PBS followed by 50, 70, 90 and 99.8% ethanol in DDI H_2O) for at least 15 min between each step. After complete dehydration, samples were chemically dried by immersion for 3 min in 1,1,1-3,3,3-hexamethyldisilazane (HMDS) with subsequent drying in the glovebox to avoid oxidation of the CuNP. Filters were stored under anoxic conditions until analysis. All fixation and dehydration steps were performed in sterile glass vials and all solutions were degassed with N_2 before transfer into the glovebox. The bacteria on the filter were not stained to avoid oxidation artifacts. The fixed samples were analyzed on a high-resolution SEM (Helios Nanolab 600i) equipped with a low voltage-high contrast (vCD) detector. The SEM was operated in immersion mode at landing energies between 0.5 and 3 keV (deceleration mode) to vary the information depth. The variation of the landing energy is achieved by setting a bias on the stage and keeping the acceleration voltage at a constant value. An advantage of this method is that more electrons can be extracted from the electron gun and that the electrons ejected from the sample are accelerated towards the vCD detector and very efficiently detected. In summary, this mode of operation allows recording BSE images at very low acceleration voltages, which would not be possible by only lowering the acceleration voltage of the microscope. For interpretation, the recorded backscattered electron (BSE) images were compared to Monte Carlo simulations performed on a Cu sphere model using CASINO 3D software code (Demers et al. 2011). No elemental analysis was carried out on electron dense particles (previously identified as CuNP) as the SEM used was not equipped with an EDX system.

DNA Extraction

Total DNA was extracted from frozen PES membrane filters (pore water DNA) as well as from the flash-frozen soil samples. Soil DNA was extracted from 5 g of soil after Zhou et al. (1996). DNA extracts were further purified with the QIAEX II gel extraction kit (Qiagen, Hilden, Germany) following the protocol of the manufacturer. Pore water DNA was extracted from PES membrane filters using the PowerSoil DNA isolation kit (MoBio Laboratories, Carlsbad, CA) following the manufacturer's instructions.

DGGE

We performed DGGE (denaturing gradient gel electrophoresis) in order to compare the microbial community diversity within the pore water and soil matrix at different periods of incubation. To target general bacterial 16S rRNA genes, we used the standard primers 341F-GC (Muyzer et al. 1993) and 907R (DeLong et al. 2006) for PCR amplification. A detailed description of PCR conditions and the DGGE setup is provided as Supplemental Content. For image acquisition and comparative analysis of DGGE banding patterns, gels were stained with silver nitrate. Subsequently, preparative gels were stained with ethidium bromide and the most prominent DGGE bands were excised. The excised DGGE bands were re-amplified with the aforementioned primers (without GC clamp), cloned, and sequenced. Because of the lower sensitivity of DNA staining with ethidium bromide compared to silver nitrate, not all DGGE bands visible on a $AgNO_3$-stained gel (Figure 4) were also visible under UV-illumination after ethidium bromide staining, and therefore, could not be excised for further analysis.

16S rRNA Gene Clone Library

For the 16S rRNA gene clone library construction, the DNA from the pore water sample collected after 4 days of flooding was PCR-amplified with the general primers GM3-8F (Muyzer et al. 1995) and 1392R (Lane et al. 1985) for bacterial 16S rRNA gene fragments. A description of the PCR reaction mix and thermo cycler program is provided as Supplemental Content. Duplicate PCR products were purified with the Wizard PCR Clean-Up System (Promega, Madison, WI) and pooled after purification. PCR products were cloned using the TOPO TA cloning kit and *E. coli* TOP10 competent cells (Invitrogen, Carlsbad, CA). *E. coli* clones were sent for sequencing of the bacterial 16S rRNA gene plasmid inserts to Eurofins MWG Operon (Ebersberg, Germany).

Phylogenetic Analysis

For comparative phylogenetic analysis, sequences of 16S rRNA gene clones from the obtained isolate, the DGGE bands, and the 16S rRNA gene clone library were assembled and trimmed using Geneious version 5.6.5 (Biomatters, http://www.geneious.com). Almost full-length sequences were aligned online using the SINA aligner (Pruesse et al. 2012) from the SILVA rRNA database project (Pruesse et al. 2007). Sequences were analyzed with the ARB software package (version 5.2) (Ludwig et al. 2004) as recommended by Peplies et al. (2008) using version 111 of the SILVA SSURef nonredundant database (Pruesse et al. 2007). The alignment was manually refined taking the secondary structure of the 16S rRNA gene into account. The tree was constructed from

full-length sequences using the maximum likelihood algorithm implemented in ARB and a 50% positional conservation filter created for the class Clostridia. Partial sequences were added to the tree using the ARB parsimony tool. For clarity, only a selected subset of the sequences used for treeing is shown in Figure 5.

Isolation of Spore Forming Bacteria

Pore water was collected from a microcosm flooded for 4 days and processed in the anoxic glovebox. Small aliquots (0.1–0.5 mL) of unfiltered pore water were inoculated in 5 mL of GYT (glucose yeast tryptone) broth (containing 10 g glucose, 5 g tryptone, 10 g yeast extract, 0.5 g Na-thioglycolate and 20 g $CaCO_3$ per L). To minimize the headspace volume, the 15 mL glass vials were sealed just above the medium with a plug consisting of a 1:1 mix of paraffin and white petroleum jelly (Vaseline). The sealed solutions were pasteurized for 10 min at 80°C in a water bath, inducing spore formation and killing all non-spore-forming bacteria in the medium. Vials were incubated overnight on a horizontal shaker at 180 rpm at 37°C. Bacterial growth during incubation and associated CO_2 production was evidenced by the paraffin plug, which moved over several centimeters inside the glass vial as a result of increasing CO_2 pressure. After 24 hours of growth, the plug was melted above a flame in order to retrieve the liquid culture. 0.1–0.2 mL of sample was spread on GYT agar plates with an inoculation loop. Plates were incubated at 37°C in an anaerobic chamber (GasPak jar) for 3 to 4 days. Single colonies were picked and re-streaked on fresh GYT plates for isolation. Isolated colonies were re-grown in GYT broth and glycerol stocks of the liquid cultures were stored at −80°C. Parts of the picked colonies were also transferred into 50-μL sterile, DNA-free H_2O for colony PCR of the *copA* resistance gene and sequencing/classification of the 16S rRNA gene.

16S rRNA and copA Gene PCR

Isolated colonies in sterile, DNA-free H_2O were directly used as template (colony PCR) for amplification of the 16S rRNA gene using the general primers GM3-8F (Muyzer et al. 1995) and GM4-1492R (Eden et al. 1991). The PCR product was prepared for sequencing by cloning as described above.

The PCR test for the presence of *copA* genes in the isolates was based on primers developed by De la Iglesia et al. (2010). A new pair of primers was designed that matched the *C. beijerinckii copA* gene (Cbei_4802_879F 5′-AGCGCTAATGGGGTTAGCACCT-3′; Cbei_4802_1386R 5′-TGCAAGGCCTAATGCACACGGA-3′) and that was subsequently tested on all *Clostridium* sp. isolates (previously identified by 16S rRNA gene amplification and sequencing).

Nucleotide Sequence Accession Numbers

The partial 16S rRNA gene sequences, retrieved from excised DGGE bands and the 16S rRNA gene clone library, have been deposited in GenBank under accession numbers HG421298 to HG421319 and HG421320 to HG421408. The 16S rRNA gene and *copA* gene sequences of the obtained isolate have the accession numbers HG326188 and HG323825.

Results

In earlier studies with soil from the same site at the river Mulde, we observed colloidal Cu mobilization prior to sulfate reduction, with a peak concentration of colloidal Cu after 8 days of flooding at 14°C (Hofacker et al. 2013b). TEM analysis of the colloidal fraction revealed CuNP associated with planktonic bacteria (Figure 1). Formation of CuNP associated with planktonic bacteria was also observed during soil incubations at 23 and 5°C, with maximal colloidal Cu concentrations after 4 and ~16 days of flooding, respectively (Hofacker et al. 2013b; Weber et al. 2009a). In these previous studies, however, the identity of the CuNP-forming bacteria and the exact location of CuNP formation relative to the bacterial cell surface have not been determined.

Electron Microscopy of Cell-Associated CuNP

In this study, analogous microcosm flooding experiments were conducted to investigate soil pore water bacteria. To clarify the location of CuNP formation, the pore water bacteria were studied by SEM. Total cell counts (1907 cells), derived from multiple SEM images, revealed that about 20% of all cells carried CuNP (Supplementary Figure S1). Images of a single pore water bacterium (recorded at landing energies of 0.5 and 1.0 keV (Figure 2a–b) corresponding to a very limited information depth of the ejected electrons) revealed an uneven bacterial surface that was free of CuNP. At increased landing energies (2.0 and 3.0 keV, Figure 2c–d) corresponding to increased information depths of the electrons, bright spots became increasingly visible that corresponded to CuNP. This trend suggested that the CuNP were below the outermost surface of the cell.

To further assess the depth of the particles in relation to the bacterial cell surface, we compared the recorded backscattered electron (BSE) images (Figure 2a–d) to calculated BSE images derived from Monte Carlo simulations of the interaction of the electron beam with CuNP of different sizes located at different depths within the bacteria (Figure 2e–h). The Monte Carlo simulations were performed using the CASINO 3D software code (Demers et al. 2011). For landing energies of 0.5, 1, 2, and 3 keV, BSE images were calculated for 20, 40, and 80 nm-sized spherical CuNP at depths of 0, 50, and 100 nm below the outermost surface (Figure 2e–h). For the cell wall layer, we assumed a peptidoglycan structure with a molecular formula of $C_{40}H_{78}N_8O_{28}$ (*N*-acetylglucosamine and *N*-acetylmuramic acid and a 5 amino acids peptide chain, namely alanine (3), glutamic acid and meso-diaminopimelic acid) (Young 2011) and a density of 1.3 g/cm^3 (Scherrer et al. 1977).

The simulations show that CuNP of all sizes are detected at all landing energies when present at the surface of the peptidoglycan layer. The simulations further show that higher

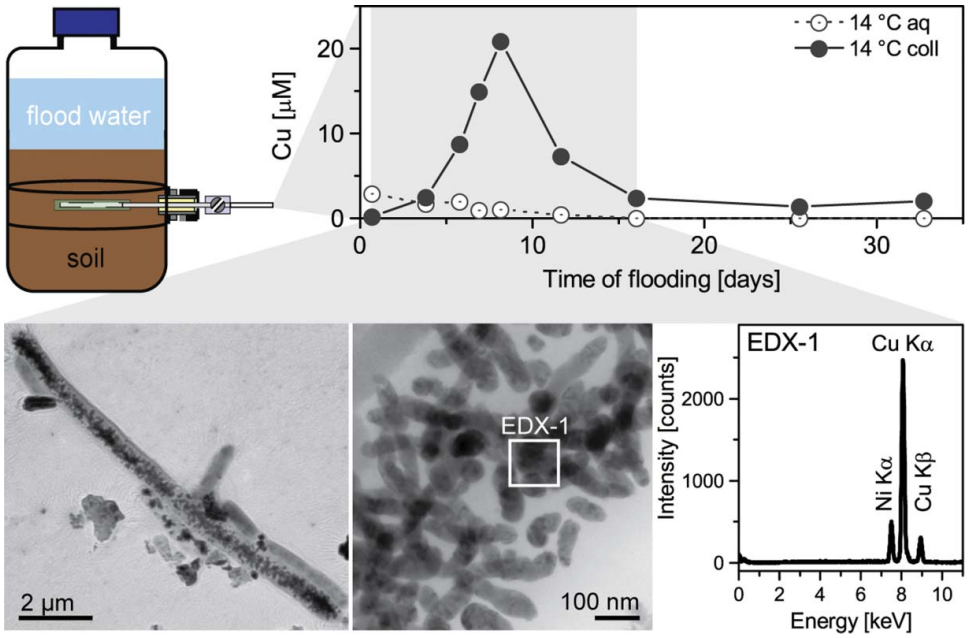

Fig. 1. Microcosm setup, colloidal, and dissolved Cu concentrations in pore water during soil flooding at 14°C and TEM images of CuNP-bearing bacteria with EDX analysis of nanoparticles. The CuNP associated with bacteria (TEM images) were primarily observed during the phase of highest colloidal Cu concentrations (shaded in gray). Pore water Cu data at 14°C from Hofacker et al. (2013b). Nanoparticles were analyzed on Ni grids and were identified as pure CuNP, no S was detected. The missing Cu Lα line (0.9 keV) in the EDX spectrum was caused by a detector failure in the energy range <2 keV, which did not affect the S Kα line (2.3 keV).

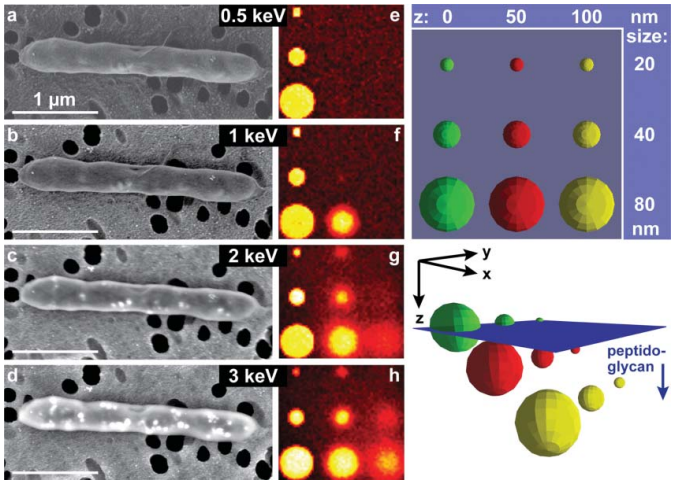

Fig. 2. Backscattered electron (BSE) images of a bacterium with CuNP on a Au-coated polycarbonate membrane filter surface collected at electron landing energies of 0.5 keV (a), 1 keV (b), 2 keV (c) and 3 keV (d), corresponding to an increasing information depth. To estimate the depth of the CuNP below the cell surface, BSE images for landing energies from 0.5 to 3.0 keV and for 20, 40, and 80 nm-sized CuNP with centers at depths of 0, 50, and 100 nm within a peptidoglycan matrix ($C_{40}H_{78}N_8O_{28}$; density 1.3 g/cm^3) (Scherrer et al. 1977) were calculated using the CASINO 3D software code (Demers et al. 2011) (e-h).

electron landing energies are required to detect smaller particles at greater depths. Even at the highest experimental landing energy of 3 keV, only the 80-nm CuNP would be detected when present at a depth of 100 nm below the surface of the peptidoglycan layer. Taking into account that most of the CuNP detected in the bacterium (Figure 2a–d) and measured at 3 keV were between 40 and 90 nm, the comparison of the simulations with our experimental results at different landing energies suggests that the centers of most CuNP were located at around 50 nm depth below the outermost cell surface.

Further complementary evidence for CuNP within bacterial cells was obtained from stereomicroscopy (Supplementary Figure S2) as the outermost surface is free of CuNP. Additional SEM images collected on the same sample revealed rod-shaped CuNP-bearing bacteria with elongated shape and terminal spores (Figure 3). This type of elongation of the vegetative cells (2- to 10-fold) at the onset of sporulation represents one characteristic sporulation behavior of Clostridia (Wiegel et al. 2006).

Microbiological Characterization of Pore Water Bacteria

We performed additional microcosm experiments to study the bacterial pore water community in more detail and to identify the CuNP-forming bacteria. Denaturing gradient gel electrophoresis (DGGE) was used to characterize compositional shifts of the microbial community in the pore water

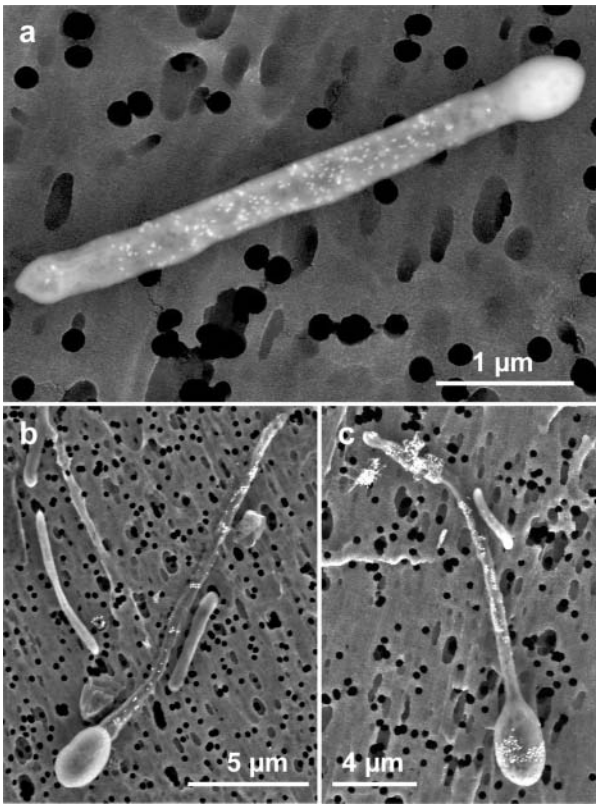

Fig. 3. Backscattered electron (BSE) images of CuNP-bearing elongated bacteria with terminal spores. (a) CuNP-bearing bacterium with a small terminal spore at an early stage of sporulation. (b, c) CuNP-bearing bacteria elongated up to ~15 μm with terminal spores of ~2 μm length.

and the soil matrix during flooding at 5–23°C. Based on SEM images, we estimated that about 20% of the bacterial cells suspended in the pore water carried CuNP (Supplementary Figure S1). DGGE with broad-specificity bacterial 16S rRNA gene primers was therefore expected to allow identification of shifts in the microbial community composition related to CuNP formation if the affected community members accounted for at least 1% of the total microbial community. DGGE-derived DNA banding patterns for seven pore water samples and the respective soil samples are shown in Figure 4. DNA banding patterns were compared for samples from the 23°C experiment at day 0.1 (initial flooding), day 4 (maximal Cu concentration prior to sulfate reduction), day 6 (during sulfate reduction), and day 26 (after complete sulfate reduction), and for samples from the 14°C experiment at day 26 (after complete sulfate reduction), and from the 5°C experiment at day 34 (during sulfate reduction). Shortly after flooding, the banding patterns of pore water DNA were very similar (b,c,g), whereas major changes in the banding patterns occurred after complete sulfate reduction (d,e). Notably, the bands dominating shortly after flooding disappeared after complete sulfate reduction, implying that only few of the bacteria involved in CuNP formation were still remaining in the pore water. The banding patterns of soil DNA samples were similar for all temperatures (ds-gs). The dominant bands of the pore water samples, however, were hardly visible, suggesting that the bacteria dominating in the soil pore water were different from the overall soil microbial community.

Three dominant gel bands of three pore water samples (b, c,g), mostly from samples of highest CuNP concentration, were visible on ethidium bromide-stained gels and could be excised, re-amplified, cloned, and sequenced. Three clones

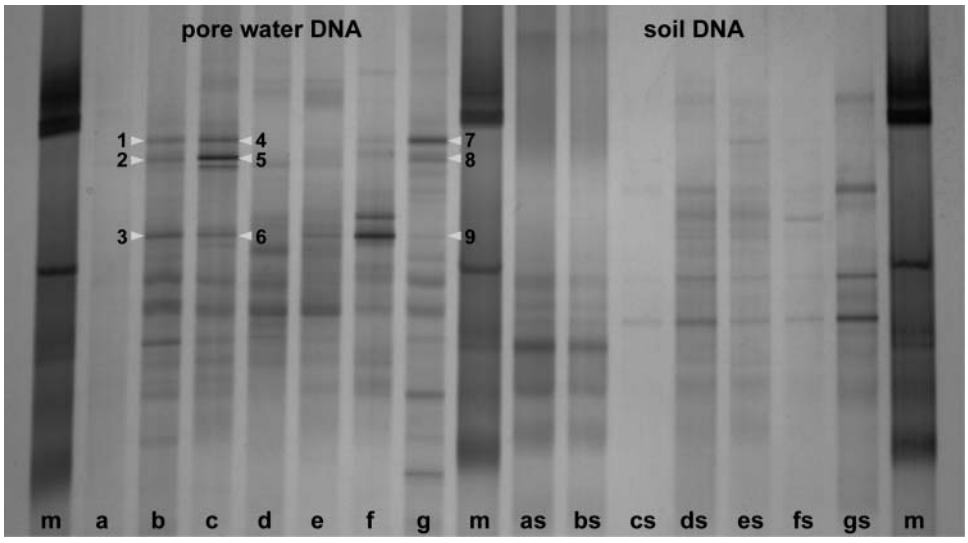

Fig. 4. Denaturing gradient gel electrophoresis (DGGE) analysis of extracted pore water and soil DNA to compare the microbial community diversity in the pore water and soil over time of flooding at 5–23°C. Seven samples of pore water DNA (a-g) and the corresponding soil DNA (as-gs) are shown. DNA was analyzed from the 23°C experiment at day 0.1 of flooding (a/as), day 4 (b/bs), day 6 (c/cs) and day 26 (d/ds), from the 14°C experiment at day 26 (e/es), from the 5°C experiment at day 33, and from a 23°C experiment with soil I used in previous experiments (Hofacker et al. 2013b; Weber et al. 2009a; Weber et al. 2009b) at day 4 (g/gs). Marker lanes are indicated by "m." All DGGE bands were 99 to 100% similar to *Clostridium* spp., except for one clone from band No. 3 which was 100% similar to *Geobacter* spp.

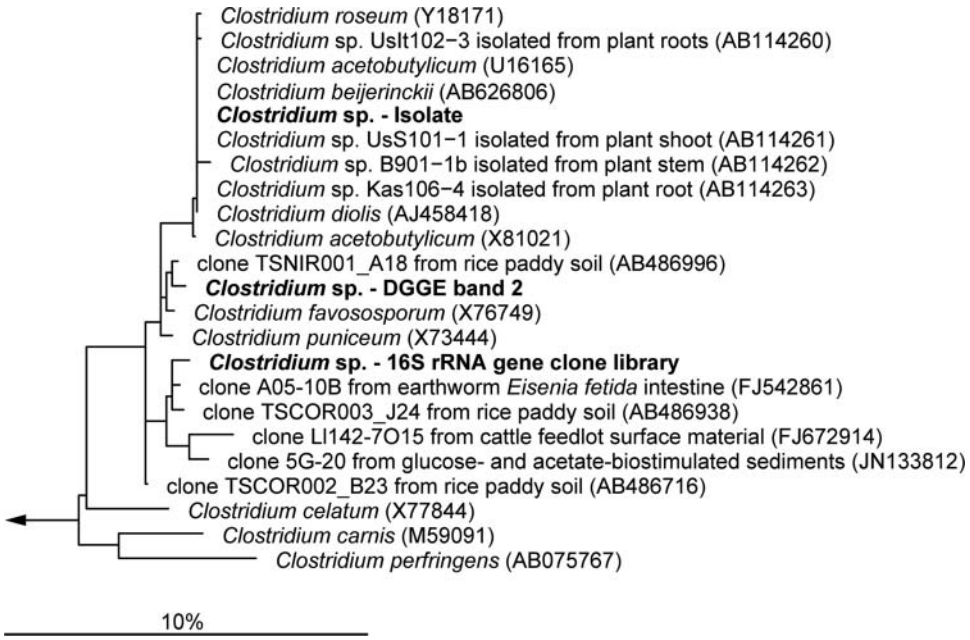

Fig. 5. Phylogenetic affiliation of the obtained *Clostridium* sp. isolate, the sequenced DGGE band 2 and one representative 16S rRNA gene clone from the 16S rRNA gene clone library to selected sequences of the class Clostridia based on comparative 16S rRNA gene analysis. Sequences of the isolate, the DGGE band and the 16S rRNA gene clone are highlighted in bold. The bar represents 10% estimated phylogenetic divergence.

per DGGE band were sequenced. All but one obtained sequences revealed 99–100% sequence similarity to *Clostridium* sp. 16S rRNA gene sequences in public databases across all samples (No. 1, 2, 4, 5, 6, 7, 8 and 9). Only one clone of DGGE band No. 3 showed 100% sequence similarity to a 16S rRNA gene sequence of *Geobacter* sp.

For further identification of the CuNP-forming bacteria, we constructed a 16S rRNA gene clone library from the pore water sample of day 4 after flooding from the 23°C experiment (Supplementary Table S1). Based on evidence from SEM analysis of CuNP-bearing bacteria with terminal spores and the abundance of *Clostridium* sp. among the sequenced DGGE bands, we isolated spore forming bacteria by pasteurization and classical microbiological plating techniques. In total, we obtained 40 isolates of which we PCR-amplified and sequenced the 16S rRNA gene. About 24% of all 16S rRNA gene clone sequences from the 16S rRNA gene clone library and all 40 isolates were classified as *Clostridium* sp.

The obtained 16S rRNA gene clone sequences from the 16S rRNA gene clone library, the isolates and the DGGE bands were used for comparative phylogenetic analysis. One representative 16S rRNA gene clone sequence obtained by each approach is shown with selected sequences of known isolates and other environmental clones of the class Clostridia in Figure 5. The obtained *Clostridium* isolate was nearly identical (99.9% sequence identity) to 16S rRNA gene sequences of *Clostridium beijerinckii*, *Clostridium acetobutylicum*, *Clostridium roseum*, and *Clostridium diolis* (no horizontal line between the species that indicate phylogenetic divergence) and therefore cannot be further distinguished based on 16S rRNA gene sequence analysis alone. The identified *Clostridium* sequence from the DGGE band No. 2 (Figure 4) and the *Clostridium* sequence from the 16S rRNA gene clone library clustered closely to the isolate. Because the 16S rRNA gene sequence obtained from the isolate is a nearly full-length sequence, while the other two sequences are partial sequences (500 and 900 bases, respectively), the phylogenetic affiliation of the isolate sequence was the most stable. Comparative sequence analysis and isolation results, therefore, both confirmed the occurrence and numerical relevance of *Clostridium* sp. in the soil pore water during CuNP formation, in line with the sporulation behavior observed by electron microscopy.

The *Clostridium* sp. isolate was tested for carrying *copA* genes, i.e., copper resistance genes that handle cytoplasmic Cu^+ efflux. All 40 isolates were tested for *copA* genes with primers developed by De la Iglesia et al. (2010), but no positive amplification was observed. Analysis of the *copA* gene sequence of *Clostridium beijerinckii* NCIMB 8052^T revealed significant gene sequence differences at the primer binding sites of the primer developed by De la Iglesia et al. (2010). The use of optimized primers for the *copA* gene sequence of *C. beijerinckii* amplified a fragment of the *copA* gene of all isolates (Supplementary Figure S3). Sequencing of the amplified *copA* gene fragment proved that the isolated *Clostridium* sp. strain carries a *copA* gene and, thus, the genetic potential for actively pumping out Cu^+ from the cytoplasm into the periplasm.

Discussion

CuNP Formation by a Clostridium Species

The presented results of classical microbiological isolation, molecular biology, and electron microscopy provide strong

evidence for CuNP formation by a Gram-positive *Clostridium* species. Until now, attempts to directly observe CuNP formation in cell suspensions of the obtained *Clostridium* isolate in Cu^{2+}-amended MES buffer (2-(N-morpholino)ethanesulfonic acid, pH 6) were unsuccessful, which may be due to different conditions in laboratory cultures compared to natural pore water. Additional molecular labeling/staining of Clostridia (e.g., using specific oligonucleotide probes in fluorescence *in situ* hybridization experiments) for simultaneous microscopic visualization and identification of cells and CuNP was not feasible, because chemical treatment of soil pore water samples for cell fixation, cell permeabilization, and probe hybridization alters the redox chemistry of the environmental sample (Schädler et al. 2008) and can affect CuNP stability (Pacioni et al. 2013) and cell association.

Nevertheless, multiple lines of evidence suggest that Clostridia are involved in CuNP formation: (i) Most 16S rRNA gene clone sequences from pore water bacteria during CuNP formation were affiliated with the genus *Clostridium* (Collins et al. 1994; Wiegel et al. 2006) and were most similar to *Clostridium beijerinckii*, *Clostridium acetobutylicum*, *Clostridium roseum*, and *Clostridium diolis*, (ii) about 20% of the porewater bacteria at this stage were observed to form CuNP by SEM analysis, and (iii) electron microscopy images revealed strongly elongated, rod-shaped CuNP-bearing bacteria (Figure 1) that develop terminal spores (Figure 3). *Clostridium* species are known to elongate to 2–10 times the usual length of their vegetative cells at the onset of sporulation before spores are even visible (Wiegel et al. 2006). The observed elongated cells with terminal spores are thus in line with one characteristic sporulation behavior of *Clostridium* species, although the relation between sporulation types and specific bacterial species or genera is not unique (Wiegel et al. 2006).

Metallic nanoparticle formation has been recently observed for Gram-positive *Clostridium pasteurianum* BC1 and *C. butyricum* reducing Pd^{2+} to Pd^0-nanoparticles (Chidambaram et al. 2010; Hennebel et al. 2011). In addition, Gram-positive *Bacillus* species have been shown to reduce Au^{3+} to Au^0-nanoparticles (Beveridge and Murray 1980; Reddy et al. 2010) and Ag^+ to Ag^0-nanoparticles (Reddy et al. 2010), and *Lactobacillus lactis* to form metallic Au, Ag and AuAg alloy nanoparticles (Nair and Pradeep 2002).

Location and Mechanism of Bacterial CuNP Formation

Standard techniques commonly used to visualize the association of bacterial cells with their biomineralization products by TEM proved unsuitable in this study because of the sensitivity of CuNP to oxidative dissolution (Pacioni et al. 2013) during fixation, staining, and ultramicrotomy (even when omitting staining with OsO_4, a strong oxidant). However, comparison of SEM images recorded at increasing landing energies with calculated BSE images derived from Monte Carlo simulations for spherical CuNP of different diameters at different depths within a peptidoglycan layer, suggested that the centers of the particles were located at ~50 nm below the outermost cell surface (Figure 2). For *B. subtilis* strain 168 a cell wall thickness of ~55 nm was reported, with a low-density inner wall zone (periplasm, 22.3 ± 4.8 nm) and a high-density outer wall zone (peptidoglycan layer, 33.3 ± 4.7 nm) (Matias and Beveridge 2005). Hayhurst et al. (2008) found the cell wall of *B. subtilis* to have a regular structure with ~53 nm wide peptidoglycan helical cables (53 ± 12 nm) running across the short axis of the cell. Assuming the cell wall of *Clostridium* sp. to exhibit a similar structure and thickness, we suggest CuNP to form in the periplasm in the proximity of the inner membrane. We cannot rule out the existence of an outermost S-layer, which has been described for several bacteria in the size range of 5–20 nm (Sleytr et al. 2007). However, even if the *Clostridium* species carried an S-layer of similar thickness, our results would still be in line with CuNP forming in the periplasm. Ag^0 nanoparticle formation in the periplasm at the inner membrane was also observed in culture experiments with the Gram-negative *S. putrefaciens* CN32 (Weisener et al. 2008).

In previous work, CuNP on suspended bacteria were proposed to form by disproportionation of Cu^+ released by the bacteria via a detoxification mechanism (Weber et al. 2009a) based on the following findings: (i) High chloride levels preventing Cu^0 formation via disproportionation by stabilizing Cu^+, (ii) spectroscopic data suggesting colloidal Cu at the onset of soil flooding to be dominantly Cu^+ in a trigonal coordination similar to bacterial Cu transport and resistance proteins, and (iii) inhibition of CuNP formation after addition of a protein synthesis inhibitor. Our results revealed that isolated *Clostridium* sp. from the pore water possessed *copA* genes and therefore the genetic potential for cytoplasmic Cu^+ efflux to maintain low levels of Cu in the cytoplasm. The importance of CopA P_{1B}-type ATPase has been mainly shown for Gram-negative, aerobic bacteria such as *E. coli* (Rensing et al. 2000), but the expression of *copA* was also important for Cu detoxification of *S. oneidensis* during anaerobic growth (Toes et al. 2008). The presence of the *copA* gene together with the formation of CuNP in the periplasm at the inner membrane indicate that the previously suggested mechanism of Cu^+ efflux and subsequent disproportionation to Cu^0 and Cu^{2+} (Weber et al. 2009a) may indeed be an important pathway for CuNP formation in soils.

Role of Fermenting Bacteria in Metal Cycling in Floodplain Soils

Fermentative bacteria (e.g., Clostridia) play an important role in soil organic matter decomposition under anaerobic conditions. Their role in metal reduction, however, has rarely been studied (Inglett et al. 2011). Gram-positive fermenting bacteria were shown to be capable of indirectly reducing ferric iron (Fe^{3+}) by reduction of humic acids, which can then transfer electrons onto Fe^{3+} (Benz et al. 1998). In freshwater sediments, fermenting bacteria were found to be important in humic acid reduction, showing that they may be relevant for electron transfer onto Fe^{3+} or to other metals (Kappler et al. 2004). Recently, Gram-positive dissimilatory metal reducing bacteria (DMRB) have been described and were even shown to be dominant in some environments (Slobodkin 2005; Wrighton et al. 2011). Carlson et al. (2012) found that *Thermincola potens* (Gram-positive bacterium that couples acetate oxidation to hydrous ferric oxide reduction (HFO) or

anthraquinone-2,6-disulfonate (AQDS) reduction) cell surface-localized redox-active multiheme *c*-type cytochromes are involved in dissimilatory metal reduction. Taken together, these findings support our observations that fermenting bacteria might be involved in anoxic metal cycling in soils.

The genus *Clostridium* forms one of the largest taxa among the Gram-positive bacteria. Given their widespread distribution, Clostridia can be expected to play an important role in metal reduction and metal biogeochemical cycling under anoxic conditions in waterlogged soils. Inglett et al. (2011) isolated and identified a Cr^{6+}-reducing *Clostridium chromiireducens* sp. nov. from a Cr^{6+}-contaminated wetland soil, also capable of Fe^{3+} reduction via electron shuttles. Based on 16S rRNA gene sequence comparison this species was most similar to *C. beijerinckii* DSM 791^T and C. roseum DSM 51^T. The *Clostridium* sp. isolate found in this study is closely related to very similar strains based on comparative 16S rRNA gene sequence analysis. This suggests that we found a *Clostridium* group I species that might be well adapted to metal stress in a contaminated floodplain soil. Assuming that the band intensities are indicative of relative species abundance, *Clostridium* sp. could account for a relative large fraction of the pore water microbial community. Their flagella-based motility enables them to engage in a pore water "planktonic" lifestyle. Furthermore their ability of sporulation makes them ideal organisms for contaminated floodplains because sporulation helps them to survive oxic and dry periods or metal stress as spores. In conclusion, the results presented in this study strongly suggest that Clostridia play an important role in copper redox cycling in periodically waterlogged soils.

Acknowledgments

Karin Stögerer is acknowledged for her help with microbiological analyses and for performing parts of the molecular microbiology work. Kurt Barmettler is acknowledged for his support in the Soil Chemistry Laboratory at ETH. We thank the electron microscopy center at ETH Zurich (EMEZ) for providing TEM facilities and Philippe Gasser for his assistance at the SEM. Fabian Gramm is acknowledged for the red cyan anaglyph images taken at CM12 at EMEZ.

Funding

This research benefitted from an exchange grant within the ESF Research Networking Program FIMIN, which is gratefully acknowledged. The study was financially supported by ETH Zurich, Eawag and University of Tübingen.

Supplemental Material

Supplemental data for this article can be accessed on the publisher's website.

References

Arguello JM, Eren E, Gonzalez-Guerrero M. 2007. The structure and function of heavy metal transport P_{1B}-ATPases. Biometals 20:233–248.

Banci L, Bertini I, McGreevy KS, Rosato A. 2010. Molecular recognition in copper trafficking. Nat Prod Rep 27:695–710.

Benz M, Schink B, Brune A. 1998. Humic acid reduction by *Propionibacterium freudenreichii* and other fermenting bacteria. Appl Environ Microbiol 64:4507–4512.

Beveridge TJ, Murray RGE. 1980. Sites of metal deposition in the cell wall of *Bacillus subtilis*. J Bacteriol 141:876–887.

Carlson HK, Iavarone AT, Gorur A, Yeo BS, Tran R, Melnyk RA, Mathies RA, Auer M, Coates JD. 2012. Surface multiheme *c*-type cytochromes from *Thermincola potens* and implications for respiratory metal reduction by Gram-positive bacteria. Proc Natl Acad Sci 109:1702–1707.

Chidambaram D, Hennebel T, Taghavi S, Mast J, Boon N, Verstraete W, van der Lelie D, Fitts JP. 2010. Concomitant microbial generation of palladium nanoparticles and hydrogen to immobilize chromate. Environ Sci Technol 44:7635–7640.

Collins MD, Lawson PA, Willems A, Cordoba JJ, Fernandez-Garayzabal J, Garcia P, Cai J, Hippe H, Farrow JAE. 1994. The phylogeny of the genus *Clostridium*: Proposal of five new genera and eleven new species combinations. Int J Syst Bacteriol 44:812–826.

De la Iglesia R, Valenzuela-Heredia D, Pavissich JP, Freyhoffer S, Andrade S, Correa JA, Gonzalez B. 2010. Novel polymerase chain reaction primers for the specific detection of bacterial copper P-type ATPases gene sequences in environmental isolates and metagenomic DNA. Lett Appl Microbiol 50:552–562.

DeLong EF, Preston CM, Mincer T, Rich V, Hallam SJ, Frigaard NU, Martinez A, Sullivan MB, Edwards R, Brito BR, Chisholm SW, Karl DM. 2006. Community genomics among stratified microbial assemblages in the ocean's interior. Science 311:496–503.

Demers H, Poirier-Demers N, Couture AR, Joly D, Guilmain M, de Jonge N, Drouin D. 2011. Three-dimensional electron microscopy simulation with the CASINO Monte Carlo software. Scanning 33:135–146.

Eden PA, Schmidt TM, Blakemore RP, Pace NR. 1991. Phylogenetic analysis of *Aquaspirillum magnetotacticum* using polymerase chain reaction-amplified 16S rRNA-specific DNA. Int J Syst Bacteriol 41:324–325.

Finney LA, O'Halloran TV. 2003. Transition metal speciation in the cell: Insights from the chemistry of metal ion receptors. Science 300:931–936.

Fulda B, Voegelin A, Ehlert K, Kretzschmar R. 2013. Redox transformation, solid phase speciation and solution dynamics of copper during soil reduction and reoxidation as affected by sulfate availability. Geochim Cosmochim Acta 123:385–402.

Hayhurst EJ, Kailas L, Hobbs JK, Foster SJ. 2008. Cell wall peptidoglycan architecture in *Bacillus subtilis*. Proc Natl Acad Sci 105:14603–14608.

Hennebel T, Van Nevel S, Verschuere S, De Corte S, De Gusseme B, Cuvelier C, Fitts JP, Van der Lelie D, Boon N, Verstraete W. 2011. Palladium nanoparticles produced by fermentatively cultivated bacteria as catalyst for diatrizoate removal with biogenic hydrogen. Appl Microbiol Biotechnol 91:1435–1445.

Hofacker AF, Voegelin A, Kaegi R, Kretzschmar R. 2013a. Mercury mobilization in a flooded soil by incorporation into metallic copper and metal sulfide nanoparticles. Environ Sci Technol 47:7739–7746.

Hofacker AF, Voegelin A, Kaegi R, Weber F-A, Kretzschmar R. 2013b. Temperature-dependent formation of metallic copper and metal sulfide nanoparticles during flooding of a contaminated soil. Geochim Cosmochim Acta 103:316–332.

Inglett KS, Bae HS, Aldrich HC, Hatfield K, Ogram AV. 2011. *Clostridium chromiireducens* sp. nov., isolated from Cr(VI)-contaminated soil. Int J Syst Evol Microbiol 61:2626–2631.

Kappler A, Benz M, Schink B, Brune A. 2004. Electron shuttling via humic acids in microbial iron(III) reduction in a freshwater sediment. FEMS Microbiol Ecol 47:85–92.

Lane DJ, Pace B, Olsen GJ, Stahl DA, Sogin ML, Pace NR. 1985. Rapid determination of 16S ribosomal RNA sequences for phylogenetic analyses. Proc Natl Acad Sci 82:6955–6959.

Lovering TS. 1927. Organic precipitation of metallic copper. US Geol Surv Bull 795-C:45–52.

Ludwig W, Strunk O, Westram R, Richter L, Meier H, Yadhukumar, Buchner A, Lai T, Steppi S, Jobb G, Forster W, Brettske I, Gerber S, Ginhart AW, Gross O, Grumann S, Hermann S, Jost R, Konig A, Liss T, Lussmann R, May M, Nonhoff B, Reichel B, Strehlow R, Stamatakis A, Stuckmann N, Vilbig A, Lenke M, Ludwig T, Bode A, Schleifer KH. 2004. ARB: A software environment for sequence data. Nucl Acids Res 32:1363–1371.

Macomber L, Imlay JA. 2009. The iron-sulfur clusters of dehydratases are primary intracellular targets of copper toxicity. Proc Natl Acad Sci 106:8344–8349.

Manceau A, Nagy KL, Marcus MA, Lanson M, Geoffroy N, Jacquet T, Kirpichtchikova T. 2008. Formation of metallic copper nanoparticles at the soil-root interface. Environ Sci Technol 42:1766–1772.

Matias VRF, Beveridge TJ. 2005. Cryo-electron microscopy reveals native polymeric cell wall structure in *Bacillus subtilis* 168 and the existence of a periplasmic space. Mol Microbiol 56:240–251.

Muyzer G, Dewaal EC, Uitterlinden AG. 1993. Profiling of complex microbial populations by denaturing gradient gel electrophoresis analysis of polymerase chain reaction-amplified genes coding for 16S rRNA. Appl Environ Microbiol 59:695–700.

Muyzer G, Teske A, Wirsen CO, Jannasch HW. 1995. Phylogenetic relationships of *Thiomicrospira* species and their identification in deep-sea hydrothermal vent samples by denaturing gradient gel electrophoresis of 16S rDNA fragments. Arch Microbiol 164:165–172.

Nair B, Pradeep T. 2002. Coalescence of nanoclusters and formation of submicron crystallites assisted by *Lactobacillus* strains. Cryst Growth Des 2:293–298.

Narayanan KB, Sakthivel N. 2010. Biological synthesis of metal nanoparticles by microbes. Adv Coll Interf Sci 156:1–13.

Osman D, Cavet JS. 2008. Copper homeostasis in bacteria. In: Laskin AI, Sariaslani S, Gadd GM, editors. Advances in Applied Microbiology. San Diego, CA: Academic Press. p 217–247.

Outten FW, Huffman DL, Hale JA, O'Halloran TV. 2001. The independent *cue* and *cus* systems confer copper tolerance during aerobic and anaerobic growth in *Escherichia coli*. J Biol Chem 276:30670–30677.

Pacioni NL, Filippenko V, Presseau N, Scaiano JC. 2013. Oxidation of copper nanoparticles in water: Mechanistic insights revealed by oxygen uptake and spectroscopic methods. Dalton Trans 42:5832–5838.

Park H-J, Nguyen TTM, Yoon J, Lee C. 2012. Role of reactive oxygen species in *Escherichia coli* inactivation by cupric ion. Environ Sci Technol 46:11299–11304.

Peplies J, Kottmann R, Ludwig W, Glockner FO. 2008. A standard operating procedure for phylogenetic inference (SOPPI) using (rRNA) marker genes. Syst Appl Microbiol 31:251–257.

Pruesse E, Peplies J, Glockner FO. 2012. SINA: Accurate high-throughput multiple sequence alignment of ribosomal RNA genes. Bioinformatics 28:1823–1829.

Pruesse E, Quast C, Knittel K, Fuchs BM, Ludwig WG, Peplies J, Glockner FO. 2007. SILVA: A comprehensive online resource for quality checked and aligned ribosomal RNA sequence data compatible with ARB. Nucl Acids Res 35:7188–7196.

Reddy AS, Chen CY, Chen CC, Jean JS, Chen HR, Tseng MJ, Fan CW, Wang JC. 2010. Biological synthesis of gold and silver nanoparticles mediated by the bacteria *Bacillus subtilis*. J Nanosci Nanotechnol 10:6567–6574.

Reith F, Etschmann B, Grosse C, Moors H, Benotmane MA, Monsieurs P, Grass G, Doonan C, Vogt S, Lai B, Martinez-Criado G, George GN, Nies DH, Mergeay M, Pring A, Southam G, Brugger J. 2009. Mechanisms of gold biomineralization in the bacterium *Cupriavidus metallidurans*. Proc Natl Acad Sci 106:17757–17762.

Rensing C, Fan B, Sharma R, Mitra B, Rosen BP. 2000. CopA: An *Escherichia coli* Cu(I)-translocating P-type ATPase. Proc Natl Acad Sci 97:652–656.

Schädler S, Burkhardt C, Kappler A. 2008. Evaluation of electron microscopic sample preparation methods and imaging techniques for characterization of cell-mineral aggregates. Geomicrobiol J 25:228–239.

Scherrer R, Berlin E, Gerhardt P. 1977. Density, porosity, and structure of dried cell walls isolated from *Bacillus megaterium* and *Saccharomyces cerevisiae*. J Bacteriol 129:1162–1164.

Sleytr UB, Huber C, Ilk N, Pum D, Schuster B, Egelseer EM. 2007. S-layers as a tool kit for nanobiotechnological applications. FEMS Microbiol Lett 267:131–144.

Slobodkin AI. 2005. Thermophilic microbial metal reduction. Microbiology 74:501–514.

Solioz M, Abicht HK, Mermod M, Mancini S. 2010. Response of Gram-positive bacteria to copper stress. J Biol Inorg Chem 15:3–14.

Toes ACM, Daleke MH, Kuenen JG, Muyzer G. 2008. Expression of *copA* and *cusA* in *Shewanella* during copper stress. Microbiol-SGM 154:2709–2718.

Tottey S, Harvie DR, Robinson NJ. 2005. Understanding how cells allocate metals using metal sensors and metallochaperones. Acc Chem Res 38:775–783.

Varshney R, Bhadauria S, Gaur MS, Pasricha R. 2010. Characterization of copper nanoparticles synthesized by a novel microbiological method. JOM 62:102–104.

Weber F-A, Voegelin A, Kaegi R, Kretzschmar R. 2009a. Contaminant mobilization by metallic copper and metal sulphide colloids in flooded soil. Nat Geosci 2:267–271.

Weber F-A, Voegelin A, Kretzschmar R. 2009b. Multi-metal contaminant dynamics in temporarily flooded soil under sulfate limitation. Geochim Cosmochim Acta 73:5513–5527.

Weisener CG, Babechuk MG, Fryer BJ, Maunder C. 2008. Microbial dissolution of silver jarosite: Examining its trace metal behaviour in reduced environments. Geomicrobiol J 25:415–424.

Wiegel J, Tanner R, Rainey FA. 2006. An introduction to the Family *Clostridiaceae*. In: Dworkin M, Falkow S, Rosenberg E, Schleifer K-H, Stackebrandt E, editors. The Prokaryotes. New York: Springer, p 654–678.

Wrighton KC, Thrash JC, Melnyk RA, Bigi JP, Byrne-Bailey KG, Remis JP, Schichnes D, Auer M, Chang CJ, Coates JD. 2011. Evidence for direct electron transfer by a Gram-positive bacterium isolated from a microbial fuel cell. Appl Environ Microbiol 77:7633–7639.

Young KD. 2011. Peptidoglycan. In: Encyclopedia of Life Sciences, Chichester: John Wiley & Sons, Ltd., p 1–11.

Zhou JZ, Bruns MA, Tiedje JM. 1996. DNA recovery from soils of diverse composition. Appl Environ Microbiol 62:316–322.